THERMODYNAMIC PROPERTIES OF CITRIC ACID AND THE SYSTEM CITRIC ACID–WATER

C.G. DE KRUIF, J.C. VAN MILTENBURG, A.J.J. SPRENKELS, G. STEVENS, W. DE GRAAF and H.G.M. DE WIT

Department of General Chemistry, Chemical Thermodynamics Group, State University of Utrecht, De Uithof, 3508 TB Utrecht (The Netherlands)

(Received 14 April 1982)

ABSTRACT

The binary system citric acid–water has been investigated with static vapour pressure measurements, adiabatic calorimetry, solution calorimetry, solubility measurements and powder X-ray measurements. The data are correlated by thermodynamics and a large part of the phase diagram is given. Molar heat capacities of citric acid are given from 90 to 330 K and for citric acid monohydrate from 120 to 300 K. The enthalpy of compound formation $\Delta_{com}H$ (298.15 K) = (-11.8 ± 1) kJ mole^{-1}.

INTRODUCTION

Many organic substances occurring in nature form hydrates. This means they can crystallize stoichiometrically with one or more moles of water, dependent on conditions of pressure and temperature. This hydrate formation is reflected in the phase diagram of the binary system 'organic substance–water', from which the regions of phase stability can be read.

As hydrates of organic substances play an important role in physiology and pharmacology, biological research groups show an increasing interest in their thermodynamic properties. Recently, our group received requests from three different research disciplines for the determination of properties such as solubility, stability region, transition temperatures and transition enthalpies for hydrates of calcium oxalate, citric acid and theophylline.

Our group has for many years been occupied with the determination of thermodynamic properties of organic substances by means of calorimetry and vapour pressure measurements. Apart from this, we are working on lattice energy determinations and calculations (by the atom–atom potential method). As in hydrates the water molecules appear to be almost exclusively bonded by hydrogen bridges, a comparison of their lattice energy calculation

with that for the corresponding anhydrates may contribute to a better understanding in the matter of hydrogen bridge bonding.

While working on the hydrates, we decided to study one binary system in greater detail, which could then be used as a reference system both for theoretical and experimental aspects. Because certain relations exist between a number of experimentally determined quantities, obtained by different methods, this fact enables us to make an estimation of the accuracy and consistency of the methods applied.

In this paper, a thermodynamic description of the citric acid–water binary system is given, with special attention to the phase behaviour of the stoichiometric crystalline hydrate. In addition, we will give a description of the experimental methods used and a discussion of the results obtained.

THERMODYNAMIC DESCRIPTION

In view of the (limited) mutual solubility, we may predict that the T–x phase diagram of the solid–liquid phases shows eutectic behaviour. Due to compound formation, the phase diagram will contain a second three-phase line at the peritectic temperature. So at constant pressure, the solid–liquid phase diagram will have the form of Fig. 1(a). Experimentally, the diagram can be obtained from the solubility of citric acid in water and from the three-phase line temperatures.

In addition to the solid–liquid phase diagram, we measured (at least in part) the solid–vapour and liquid–vapour equilibria. Because citric acid is less volatile than water by at least a factor of 10^9 at temperatures below 373 K, we assume water to be the only species present in the vapour phase. The system citric acid water–water vapour is monovariant and the P–x diagrams
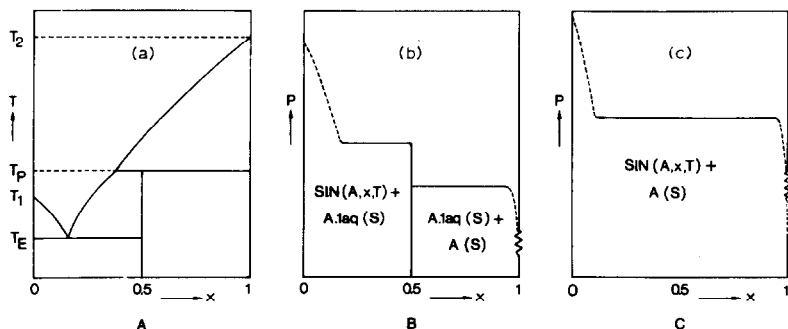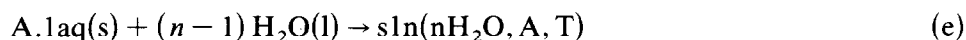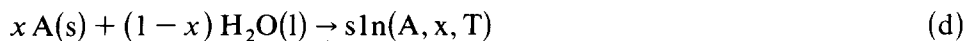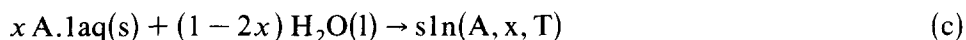

Fig. 1. (a) General features of the expected phase diagram. (b) and (c) Sketched P–x diagrams for temperatures below and above the peritectic temperature, respectively.
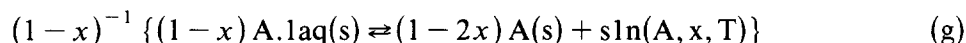
will be as sketched in Fig. 1(b) and (c). Apart from these phase diagrams, we are particularly interested in the change in values of the thermodynamic functions, when a point in the diagram is realized by mixing the pure components in appropriate quantities and at appropriate temperatures. Because we also measured some equilibria along the two-phase lines, we will write out these 'phase reactions' in a general form together with some auxilliary equations.
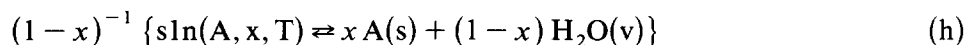
GENERAL EQUATIONS

Citric acid will be denoted by A, the hydrate by A.1aq, and a saturated solution of citric acid in water by $sln(A, x, T)$ meaning that the solution contains $(1 - x)$ moles of water and x moles of citric acid at temperature T. The diluted solution is defined by $sln(nH_2O, A, T)$, containing 1 mole of A and n ($> = 500$) moles water. For temperatures below the peritectic temperature, we may write

$$A(s) + H_2O(l) \rightarrow A.1aq(s) \tag{a}$$

$$A.1aq(s) \rightleftharpoons A(s) + H_2O(v) \tag{b}$$

$$x\,A.1aq(s) + (1 - 2x)\,H_2O(l) \rightarrow sln(A, x, T) \tag{c}$$

$$x\,A(s) + (1 - x)\,H_2O(l) \rightarrow sln(A, x, T) \tag{d}$$

$$A.1aq(s) + (n - 1)\,H_2O(l) \rightarrow sln(nH_2O, A, T) \tag{e}$$

$$A(s) + n\,H_2O(l) \rightarrow sln(nH_2O, A, T) \tag{f}$$

At the peritectic or transition temperature

$$(1 - x)^{-1}\,\{(1 - x)\,A.1aq(s) \rightleftharpoons (1 - 2x)\,A(s) + sln(A, x, T)\} \tag{g}$$

Above the peritectic temperature

$$(1 - x)^{-1}\,\{sln(A, x, T) \rightleftharpoons x\,A(s) + (1 - x)\,H_2O(v)\} \tag{h}$$

We will also make use of

$$H_2O(l) \rightleftharpoons H_2O(v) \tag{i}$$

Except for eqns. (a) and (i), we have determined the enthalpy and/or entropy changes of the respective phase reactions. By suitable combination of these quantities, others can be calculated. We will illustrate this on the enthalpy changes but it can be done for the entropy likewise.

ENTHALPY OF COMPOUND FORMATION

$$\Delta_{com} H_a = H^*(A.1aq, s) - H^*(A, s) - H^*(H_2O, l)$$

This can be found from the following quantities determined experimentally.

$$\Delta_{sat} H_d - \Delta_{sat} H_c = H(slnA, x, T) - x H^*(A, s) - (1 - x) H^*(H_2O, l)$$
$$\underline{- H(slnA, x, T) + x H^*(A.1aq, s) + (1 - 2x) H^*(H_2O, l)}$$
$$x\Delta_{com} H_a = x H^*(A.1aq, s) - x H^*(A, s) - x H^*(H_2O, l) \qquad (1)$$
$$\Delta_{com} H_a = H^*(A.1aq, s) - H^*(A, S) - H^*(H_2O, l)$$
$$\Delta_{vap} H_i - \Delta_{vap} H_b = H^*(H_2O, v) - H^*(H_2O, l)$$
$$\underline{- H^*(A, s) - H^*(H_2O, v) + H^*(A.1aq, s)}$$
$$\Delta_{com} H_a = H^*(A.1aq, s) - H^*(A, s) - H^*(H_2O, l) \qquad (2)$$
$$\Delta_{sol} H_f - \Delta_{sol} H_e = H(sln, nH_2O, A, T) - H^*(A, S) - n H^*(H_2O, l)$$
$$\underline{- H(sln, nH_2O, A, T) + H^*(A.1aq, s) + (n - 1) H^*(H_2O, l)}$$
$$\Delta_{com} H_a = H^*(A.1aq, s) - H^*(A, s) - H^*(H_2O, l) \qquad (3)$$

ENTHALPY OF SOLUTION

It can be shown that the integral enthalpy of solution at saturation concentration of citric acid is given by

$$\Delta_{sat} H_d = (1 - x)\left[\Delta_{com} H_a + \Delta_{trs} H_g\right] \qquad (4)$$

$$\Delta_{sat} H_d = (1 - x)\left[\Delta_{vap} H_i - \Delta_{vap} H_h\right] \qquad (5)$$

and similarly for the hydrate

$$\Delta_{sat} H_c = (1 - 2x) \Delta_{com} H_a + (1 - x) \Delta_{trs} H_g \qquad (6)$$

$$\Delta_{sat} H_c = \Delta_{sat} H_d - x \Delta_{com} H_a \qquad (7)$$

ENTHALPY OF TRANSITION

The enthalpy change connected with the phase transition of eqn. (g) is measured calorimetrically or evaluated from

$$\Delta_{vap}H_b' - \Delta_{vap}H_h = +H^*(H_2O,v) + H^*(A,s) - H^*(A,1aq,s)$$

$$-H^*(H_2O,v) - x(1-x)^{-1}H^*(A,s) + (1-x)^{-1}H(sln,A,x,T)$$

$$\Delta_{trs}H_g = (1-2x)(1-x)^{-1}H^*(A,s)$$
$$+ (1-x)^{-1}H(sln,A,x,T) - H^*(A,1aq,s) \qquad (8)$$

Of course other combinations are possible, but we consider those given as the most relevant ones.

EXPERIMENTAL EVALUATION

The enthalpy changes corresponding to eqns. (e)–(g) are determined by calorimetry. Absolute entropies and entropy changes are evaluated from specific heat capacity measurements. The enthalpy changes corresponding to eqns. (b) and (h) are derived from the Clausius–Clapeyron law

$$-R\,d\ln[p(H_2O)/p^0]/d(1/T) = \Delta_{vap}H \qquad (9)$$

In the treatment given above, it was assumed that all enthalpy values are determined at the same temperature. In practice, this will not be true and so we have to account for the temperature dependence of the enthalpy.

$$\Delta H(T) = \Delta H(T_0) + \int_{T_0}^{T} \Delta C_p(T)\,dT \qquad (10)$$

In most cases, it will be accurate enough to use

$$\Delta H(T) = \Delta H(T_0) + \overline{\Delta C_p}(T - T_0) \qquad (11)$$

in which $\overline{\Delta C_p}$ is the mean value in the temperature range $T-T_0$.

SAMPLES

Commercially available (Baker Analyzed, 99.8%) citric acid monohydrate (formula mass 210.12) was used. Citric acid was prepared from the hydrate by prolonged heating and evacuation at 60°C. From the mass loss, the ratio citric acid:water in the hydrate was found to be 1.00 ± 0.005.

VAPOUR PRESSURE MEASUREMENTS

These measurements were performed by a static method employing a diaphragm manometer (MKS Baratron Inc.) calibrated on a dead weight

gauge (CEC). Temperature was measured with a platinum thermometer calibrated on IPTS-68 and accurate to within 0.01 K. The experimental set-up has been described in detail previously [1]. The vapour pressure measurements as a function of temperature are fitted to the equation

$$R\ln(p/p^0) = -\Delta G^0(\theta)/\theta + \Delta H^0(\theta)(1/\theta - 1/T)$$
$$+ \Delta C_p^0(\theta)\{\theta/T - 1 + \ln(T/\theta)\} \tag{12}$$

in which p^0 is a standard pressure of 1 Pa, θ is a reference temperature, usually mid-range, while the coefficients to be evaluated, ΔG^0, ΔH^0 and ΔC_p^0, are the thermodynamic function changes on vaporization.

SOLUTION CALORIMETRY

An isoperibol calorimeter was used. About 0.2 g of sample was dissolved in 100 ml water. The corresponding enthalpy effect was evaluated from the measured temperature change and a separate specific heat determination.

Data were collected by a microcomputer and a correction for heat leak (heat leak constant = -4.7×10^{-5} s^{-1}) was applied. The performance of the apparatus was checked by measuring the heat of solution of potassium chloride. From twenty measurements, a mean heat of solution of $17,34 \pm 0.035$ kJ mole^{-1} was measured. This is in good accord with literature data of corresponding concentrations.

TABLE 1

Solubility, x, of citric acid monohydrate in water

T(K)	x (mole fraction)
290.1	0.1123
296.1	0.1233
299.2	0.1354
304.0	0.1488
304.9	0.1501
307.6	0.1559
309.0	0.1636
313.9	0.1750
317.5	0.1860
322.1	0.1923

SOLUBILITY

The solubility of citric acid (monohydrate) in water was determined by putting together appropriate and precisely weighed amounts of the acid and water in a glass tube which was then sealed off. The glass tubes were rotated in a thermostat whose temperature was raised by approximately 1 K per day. The temperature at which the crystals are completely dissolved was taken as a point of the liquidus. The results are given in Table 1.

POWDER X-RAY DIFFRACTION

These measurements were made in the temperature range 32–38°C with a heating rate of 0.2 K ks^{-1} and a film speed of 3 μm s^{-1}. The diffraction pattern of the Cu$K\alpha_1$ radiation was recorded on a Guinier–Simon camera (Enraf Nonius, The Netherlands). From the abrupt change in diffraction pattern, the transition temperature was evaluated.

ADIABATIC CALORIMETRY

The calorimeter used has been described before [2]; no alterations have been made.

RESULTS AND DISCUSSION

The molar heat capacity of citric acid monohydrate (sample mass 17.4095 g) was measured under a helium pressure of about 200 Pa. The measurements were made between 110 and 330 K. The experimental results are given in Table 2 and the calculated thermodynamic values in Table 3. A large transition, which was slightly superheated, took place at 312.1 K (see Fig. 2). The heat capacity of the sample above the transition is very large and does show a large temperature dependence. The enthalpy of transition was calculated in the usual way by taking the enthalpy increment from 298 to 321 K and subtracting the heat capacity contribution. This heat capacity was linearly extrapolated to 312.1 K using the regions from 285 to 298 K and from 321 to 333 K. The enthalpy of transition was 14.98 kJ mole^{-1}. After these measurements, the sample was cooled to 278 K and a cooling curve made. After several hours at 278 K, a gradual exothermic effect took place which is quite different from the sudden crystallisation of a supercooled liquid. After two days, a new series of measurements was made. A significant

TABLE 2

Experimental molar heat capacities, C_p

T (K)	C_p (J K^{-1} mole^{-1})	T (K)	C_p (J K^{-1} mole^{-1})	T (K)	C_p (J K^{-1} mole^{-1})	T (K)	C_p (J K^{-1} mole^{-1})
(a) *Citric acid monohydrate*							
118.23	126.79	190.46	183.38	245.09	225.29	291.86	262.21
123.81	131.25	194.67	186.23	248.69	228.16	295.05	264.31
129.24	135.63	198.82	189.61	252.26	231.06	298.21	267.36
134.53	139.90	202.92	192.33	255.79	233.77	301.34	271.02
139.69	144.09	206.96	195.67	259.30	236.62	304.44	275.35
144.74	147.92	210.97	198.56	262.77	239.52	307.50	282.28
149.68	151.76	214.93	201.83	266.21	241.71	310.48	301.15
154.53	155.73	218.83	205.17	269.63	244.55	316.22	406.97
159.28	159.24	222.70	207.76	273.02	247.38	318.58	399.46
163.96	163.07	226.53	210.83	276.37	249.91	320.88	406.27
168.55	166.64	230.32	213.63	279.70	252.15	323.16	413.19
173.06	170.12	234.07	216.66	283.01	254.77	325.40	419.78
177.51	173.73	237.78	219.54	285.42	256.71	327.62	426.56
181.88	176.90	241.45	222.60	288.66	259.19	329.80	434.56
186.20	180.14						
Second series							
288.74	258.18	303.82	279.68	316.47	403.41	324.73	418.76
292.59	262.88	307.33	324.79	319.27	401.98	327.39	427.31
296.39	267.70	309.77	788.29	322.03	410.34	330.01	436.40
300.14	273.05						
(b) *Citric acid*							
84.19	83.93	174.77	150.29	245.33	193.79	302.98	228.45
94.47	93.34	181.67	154.61	257.16	201.16	305.66	230.30
104.04	100.76	188.46	158.94	262.94	204.57	308.32	231.21
113.07	107.53	195.14	163.34	268.66	208.19	310.98	233.36
121.67	114.05	201.71	167.50	276.69	213.03	313.63	234.69
129.94	120.25	208.17	171.45	282.27	216.44	316.28	235.92
137.92	125.55	214.55	175.43	287.79	219.05	318.91	237.36
145.67	130.66	220.84	179.01	293.27	222.75	321.54	239.20
153.19	136.46	227.05	182.95	298.71	225.99	324.15	241.22
160.54	141.29	233.18	186.44	297.59	224.80	326.76	242.32
167.73	146.04	239.34	190.31	300.29	226.75	329.35	244.23

difference in the heat capacity prior to the transition and a lower enthalpy of transition (including the larger pre-effect) of 14.47 kJ mole^{-1} were found, indicating that the formation of the monohydrate from the high-temperature

TABLE 3

Calculated thermodynamic values of citric acid monohydrate

T (K)	C_p ($J\ K^{-1}$ mole^{-1})	$G - G(0)$ (J mole^{-1})	$H - H(0)$ (J mole^{-1})	$S - S(0)$ ($J\ K^{-1}$ mole^{-1})
120	128.14	−5728	7849	113.14
130	136.28	−6913	9171	123.72
140	144.28	−8202	10574	134.11
150	152.18	−9594	12056	144.34
160	159.98	−11098	13617	154.41
170	167.70	−12682	15255	164.34
180	175.37	−14375	16971	174.14
190	183.00	−16165	18763	183.83
200	190.69	−18051	20631	193.41
210	198.20	−20032	22575	202.89
220	205.82	−22108	24585	212.29
230	213.47	−24278	26691	221.60
240	221.18	−26540	28864	230.85
250	228.95	−28895	31115	240.04
260	236.81	−31341	33444	249.17
270	244.78	−33878	35851	258.26
280	252.88	−36506	38340	267.30
290	261.12	−39224	40900	276.32
300	269.52	−42032	43562	285.32
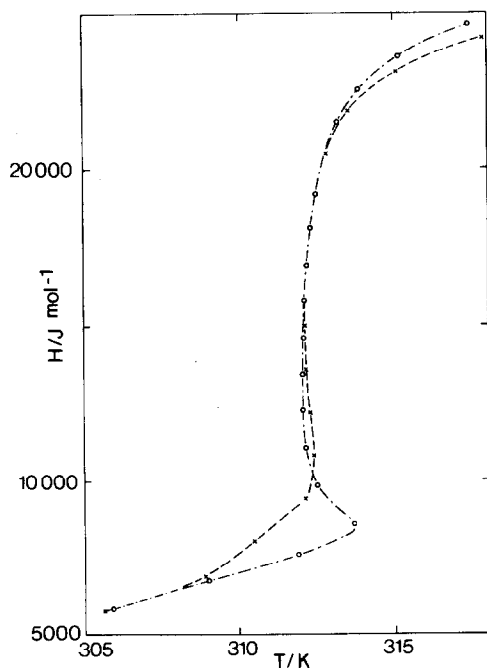
Fig. 2. The enthalpy curve by adiabatic calorimetry. ○ = first series; × = second series.

phase was not complete. In this second measurement, the superheating of the transition was only about 0.1 K.

For citric acid, a sample of 8.0608 g was used. Helium gas was admitted to a pressure of 200 Pa. Measurements were made between 80 and 330 K. As no specific heat anomaly was found in the region where the monohydrate has its transition, it is safe to assume that no hydrate was present. The experimental results are also given in Table 2, and the calculated thermodynamic values and the smoothed heat capacity values from 90 K are given in Table 4. Specific heat measurements of the monohydrate have been reported by Evans et al. [3] ranging from 10 to 298 K. Comparing our data from 90 to 298 K shows no significant difference. Our data measured with automated apparatus are more smooth, but the overall difference in enthalpy increment

TABLE 4

Calculated thermodynamic values of citric acid

T (K)	C_p ($J\ K^{-1}\ mole^{-1}$)	$G - G(90)$ $J\ mole^{-1}$)	$H - H(90)$ ($J\ mole^{-1}$)	$S - S(90)$ ($J\ K^{-1}\ mole^{-1}$)
90	90.03	0	0	0.00
100	97.79	− 50	939	9.89
110	105.36	− 198	1955	19.57
120	112.74	− 441	3045	29.05
130	119.94	− 778	4209	38.36
140	126.98	− 1207	5444	47.51
150	133.87	− 1728	6748	56.50
160	140.62	− 2337	8121	65.36
170	147.24	− 3034	9560	74.08
180	153.74	− 3818	11065	82.68
190	160.13	− 4688	12634	91.17
200	166.43	− 5641	14267	99.54
210	172.64	− 6678	15963	107.81
220	178.78	− 7797	17720	115.99
230	184.85	− 8998	19538	124.07
240	190.87	− 10278	21417	132.06
250	196.85	− 11639	23355	139.98
260	202.80	− 13078	25353	147.81
270	208.73	− 14595	27411	155.58
280	214.65	− 16189	29528	163.27
290	220.57	− 17860	31704	170.91
300	226.51	− 19607	33940	178.49
310	232.48	− 21430	36234	186.01
320	238.48	− 23327	38589	193.42
330	244.53	− 25299	41004	200.92

in this region is only 18 J mole^{-1} or less than 0.05% of the total effect. Table 3 is calculated by using the Evans values for the absolute entropy and the enthalpy at 120 K. No measurements of the heat capacity of the monohydrate above 298 K or of citric acid have been reported before.

The experimentally measured vapour pressures over the hydrate and the saturated solution are given in Table 5. After pumping a few seconds at the hydrate sample, it took several hours before the equilibrium pressure was re-established. Therefore the scatter in these data is much higher than in those of the saturated solution for which equilibrium was established in a few minutes. When the saturated solution was cooled well below the transition temperature, vapour pressures were not initially constant and were well above the equilibrium values. Only after several days equilibrium were they re-established, indicating again the slow equilibration mechanism as observed in adiabatic calorimetry. The result of fitting the experimental vapour pressure data to eqn. (12) is given in Table 6.

From the intersection of the two vapour pressure lines, the transition temperature is found to be 309.5 ± 0.5 K. The X-ray powder diffraction patterns give a transition temperature of 309.0 ± 0.5 K. This is compared

TABLE 5

Experimental water vapour pressures above citric acid monohydrate and above a saturated solution

Citric acid monohydrate			Saturated solution		
T (K)	P (Pa)	$100*\Delta \ln P *$	T (K)	P (Pa)	$100*\Delta \ln P *$
278.10	325.00	−2.01	309.77	4141.00	−0.40
282.88	521.00	2.40	314.78	5414.00	1.89
289.11	893.00	3.14	316.95	5773.00	−1.92
293.12	1212.00	0.95	321.87	7311.00	−0.73
293.75	1213.00	−4.01	322.89	7756.00	0.64
297.67	1748.00	1.77	329.30	10 109.00	−0.18
298.42	1760.00	−3.34	330.09	10 645.00	1.73
301.99	2332.00	−2.17	338.01	14 368.00	0.53
303.23	2582.00	−1.18	342.22	16 609.00	−0.59
306.15	3240.00	0.23	342.31	16 662.00	−0.58
306.17	3399.00	4.78	342.27	16 530.00	−1.26
306.42	3373.00	2.35	351.77	23 346.00	0.39
308.96	3902.00	−1.20	351.81	23 333.00	0.20
309.06	3906.00	−1.77	351.84	23 386.00	0.31

* The residuals are calculated from eqn. (12) and the coefficients given in Table 6.

TABLE 6

Experimental results and comparison with literature

Reaction	T	$\Delta G^0(T)$	$\Delta H(T)$	$\Delta C_p^0(T)$	P	Ref.
	(K)	(kJ mole^{-1})	(kJ mole^{-1})	(J mole^{-1} K^{-1})	(Pa)	
A.laq(s) $\rightleftharpoons$ A(s) + H$_2$O(v)	298.15 309.5	9.98±0.03	56.8±0.8 55.8±1.0	−93±130	1770 4100	
A.laq(s) + (n−1) H$_2$O(l) → sln(n H$_2$O, A, T)	298.15		−29.25±0.2 −29.79			7
A(s) + n H$_2$O(l) → sln(n H$_2$O, A, T)	298.15		−18.47±0.09 −22.6			8
(1−x)$^{-1}$ {(1−x) A.laq(s) $\rightleftharpoons$ (1−2x) A(s)+sln(A, x, T)}	312.1		14.98±0.02			
(1−x)$^{-1}$ {sln(A, x, T) $\rightleftharpoons$ x A(s)+(1−x) H$_2$O(v)}	333.15	5.91±0.01	36.67±0.2	−145± 35	11660	
H$_2$O(l) $\rightleftharpoons$ H$_2$O(v)	298.15 309.5	8.56±0.01	44.02±0.04 43.5±0.04	−32	3168 6060	6 6

with a literature value of 309.7 K [4,5]. The transition temperature found with the adiabatic calorimeter is 312.1 K. Although a temporary superheating of 1.5 K is observed, it is not clear where this discrepancy originates, particularly as we have used extremely low heating rates comparable with those of the X-ray powder diffraction experiments. For further calculation, we will adopt a transition temperature of 309.5 K.

The heats of solution of the hydrate and of the anhydrate were each determined eight times. In Table 6 we give the experimental results and literature values.

The values of pure water have been taken from ref. 6. Employing eqns. (2) and (3), we find for the enthalpy of compound formation as defined by eqn. (a) from vapour pressure measurements $\Delta_{com}H_a$ (298.15 K) $= -12.8 \pm 1$ kJ mole^{-1}, $\Delta_{com}H_a$ (309.5 K) $= -12.3 \pm 1$ kJ mole^{-1} and $\Delta_{com}H_a$ (298.15 K) $= -10.8 \pm 0.6$ kJ mole^{-1} from solution calorimetry. The enthalpy of transition defined by eqns. (g) and (8) is found to be $\Delta_{trs}H_g$ (309.5 K) $= 15.69 \pm 1$ kJ mole^{-1} and $\Delta_{trs}H_g$ (312.1 K) $= 14.98 \pm 0.2$ kJ mole^{-1} from vapour pressure measurements and adiabatic calorimetry, respectively.

For equilibrium (b), from the values in Table 6 we calculate $\Delta_{vap}S_b^0$ (298.15 K) $= 157.21 \pm 2.7$ J K^{-1} mole^{-1}.

Using the absolute entropies of the monohydrate and water vapour, we calculate the absolute entropy of citric acid as S^0 (s, 298.15 K) $= 252.1$ kJ^{-1} mole^{-1}. The relative value S^0 (s, 298.15 K) $- S^0$ (s, 90 K) $= 177.1$ J K^{-1} mole^{-1}. Therefore to convert the entropy values in Table 4 to absolute values they must be increased by 75 J K^{-1} mole^{-1}. So, S^0 (s, 90 K) $= 75$ J K^{-1}
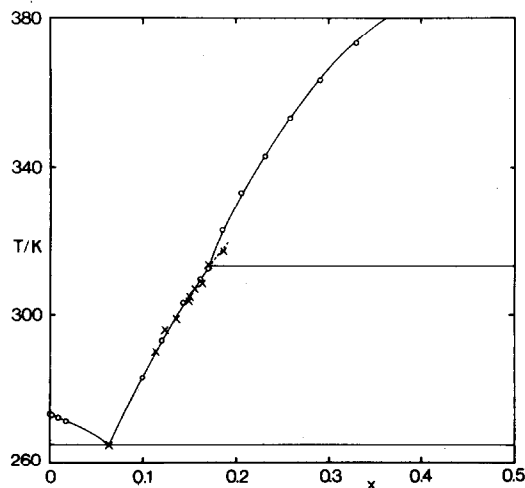

Fig. 3. The experimental phase diagram between $x = 0$ (water) and $x = 0.5$ (the hydrate). O = literature data; X = our measurements.

mole^{-1}. Of course several other thermodynamic quantities of the system citric acid–water can be calculated with the results presented here and making use of the consistent set of phase transition equations given above. We think that those given are the most interesting and useful ones.

Finally, we give in Fig. 3 the binary T–x phase diagram based on both our measurements and literature values.

REFERENCES

1 C.G. de Kruif, T. Kuipers, J.C. van Miltenburg, R.C.F. Schaake and G. Stevens, J. Chem. Thermodyn., 13 (1981) 1081.
2 R.C.F. Schaake, J.C.A. Offringa, G.J.K. van den Berg and J.C. van Miltenburg, Rec. Trav. Chim. Pays-Bas, 98 (1979) 408.
3 D.M. Evans, F.E. Hoare and T.P. Melia, Trans. Faraday Soc., 58 (1962) 1511.
4 Kirk-Othmer, Encyclopedia of Chemical Technology, Wiley, New York, 1978.
5 J.L. Marshall, J. Proc. Aust. Chem. Inst., 5 (1938) 383.
6 R.A. Robie, B.S. Hemingway and J.R. Fisher, Thermodynamic Properties of Minerals. U.S. Government Printing Office, Washington, 1978.
7 B.J. Levin, J. Phys. Chem., 59 (1955) 640.
8 International Critical Tables of Numerical Data, Vol. V, McGraw-Hill, New York, 1929.